Electronic Supplementary Material (ESI) for Nanoscale Advances.
This journal is © The Royal Society of Chemistry 2020

Supplementary Information for B_5N_5 Monolayer: A Room-temperature Light Element Antiferromagnetic Insulator

Dong Zhang[1,2] Qihua Xiong[3,4] and Kai Chang[1,2]

[1]*SKLSM, Institute of Semiconductors, Chinese Academy of Sciences, P.O. Box 912, Beijing 100083, China*

[2]*Center for Excellent in Topological Quantum Computation, University of Chinese Academy of Sciences, Beijing 100190, China*

[3]*Division of Physics and Applied Physics, School of Physical and Mathematical Sciences, Nanyang Technological University, Singapore, Singapore*

[4]*State Key Laboratory of Low-Dimensional Quantum Physics and Department of Physics, Tsinghua University, Beijing 100084, China*

1 Part I. Validation of DFT results

The band structures of monolayer B_5N_5 have been performed by various calculations, such as the rotationally invariant DFT+U approach with series of Hubbard U corrections up to 5 eV, and tunable exchange interactions within the HSE06 scheme. The antiferromagnetic insulator feature remains unchanged, and the differences between various calculations are minor. The band structures are shown in FigS.S1

Even with ultra high U values incorporated into the electronic structures calculations, the flat

band features and the values of the band gaps change little. The comparison between various calculation conditions confirm the reliability of the numerical results, thusly we take HSE06 scheme as routine procedure all through this study.

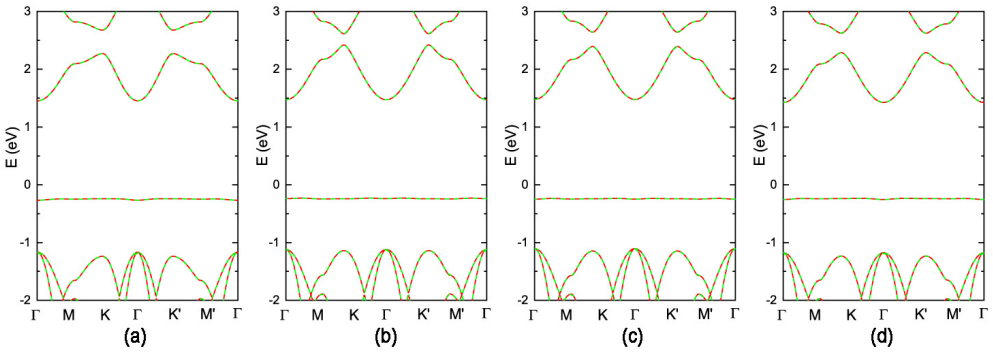

Figure S1: **Validation of DFT results.** Band structures of monolayer B_5N_5 obtained by (a) HSE06 calculation, and LDA+U calculations with (b)U_B=U_N=5 eV; J_B=J_N=0 eV. (c)U_B=U_N=3.5 eV; J_B=J_N=0.1 eV. and (d) U_B=3.5 eV; J_B=0.1 eV; U_N=0.5 eV; J_N=0.3 eV.

2 Part II. Magnetic orderings

By performing constrained DFT calculations, ferromagnetic, antiferromagnetic and intermediate magnetic orderings are calculated. Since the spatial spin distributions and density of spin states have been shown in Fig. 2 in the manuscript, here we present detailed information about each magnetic ordering as shown in FigS.S2.

In FigS.S2, the spatial spin distributions are displayed in periodic lattices, and the unitcell for each magnetic ordering is labelled with black solid lines. One can find out that, the antiferromagnetic (a) and ferromagnetic (d) orderings are computed in 1×1 unitcell. However, for the

intermediate magnetic orderings, the unitcells are $\sqrt{3} \times \sqrt{3}$ for (b) and $\sqrt{2} \times \sqrt{2}$ for (c), respectively.

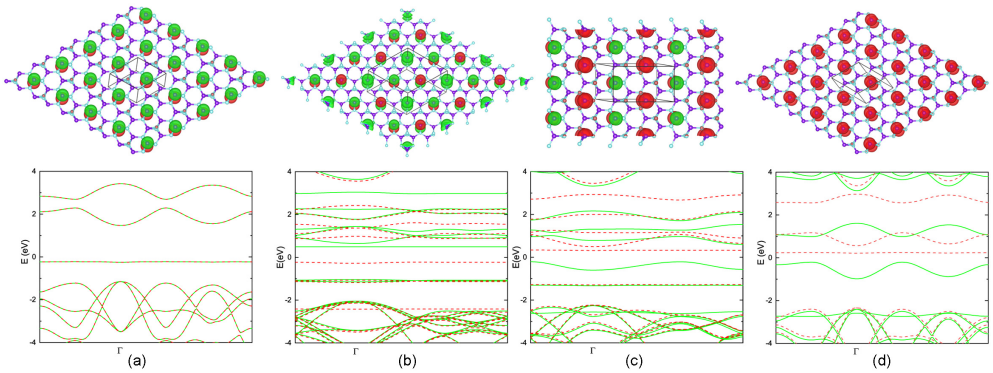

Figure S2: **Electronic structures of various magnetic orderings.** From (a) to (d), the spatial spin distributions (upper panel) and the spin resovle band structures (lower panel) are displayed in the sequence agree with Fig. 2 in the article. Each unitcell of B_5N_5 monolayers is marked with black solid lines in the upper panel, spin-up and spin-down states are shown with red and green colour codings, respectively.

Utilizing the effective magnetic Hamiltonian and by performing constrained DFT calculations with different initial magnetic orderings as shown in Fig.4. The total energy of the studied magnetic orderings can be expressed as the formula as follows;

$$E_{total} = \frac{\sum_{i=1}^{N} S_{i\downarrow} \cdot S_{i\uparrow} J_{\perp} + \sum_{u=\uparrow,\downarrow} \sum_{j=1}^{6} S_u \cdot S_{u,j} J_{\parallel}}{N} + \Delta \tag{1}$$

where N is the multiple of the calculated supercell with respect to the original unitcell, as well as the number of the magnetic dipoles. Specifically, N=1 for AFM and FM magnetic orderings, while N=3 for the intermediate model 2 and N=2 for the intermediate model 3. j=1,..,6 is the index of coordinate spin accumulated sites. And the total energies are divided by N to be compared with

equal number of atoms, and Δ is non-magnetic total energy of the unitcell. it is convenient to derive magnetic exchange coupling parameters by solving the following equations;

$$\begin{cases} E_{AFM} = (-1*1)J_{\perp} + 6*\frac{1}{2}*(1*1)J_{\parallel} + 6*\frac{1}{2}*(-1*-1)J_{\parallel} + \Delta = -75553.8meV, \\ E_{Int1} = \frac{J_{\perp}+6*J_{\parallel}}{3} + \Delta = -75532.3meV, \\ E_{Int2} = 3*J_{\parallel} + \Delta = -75520.9meV, \\ E_{FM} = (1*1)J_{\perp} + 6*\frac{1}{2}*(1*1)J_{\parallel} + 6*\frac{1}{2}*(1*1)J_{\parallel} + \Delta = -75400.4meV, \end{cases} \tag{2}$$

3 Part III. External Strain

Interfacial strains are common in solid-state devices and also provide a controllable method to tune properties of materials. Considering possible application as monolayer antiferromagnet in vdW heterostructure devices, the response of magnetic orderings of B_5N_5 to interfacial strains are investigated. In this section, biaxial strain are modelled with deformed monolayers, within a presumption that, the volume of the monolayer keep constant under external strain. To be specifically, the biaxial tensile strain increases in-plane lattice constants but reduces the out-plane lattice constant, and the deformation of monolayers are quite opposite under biaxial compressive strains.

From our calculations, the tensile strains increase the band gap and keep the intralayer ferromagnetic and interlayer ferromagnetic (A-type antiferromagnet) feature remains. While the consequences of compressive strains are more complicated, the A-type antiferromagnetic feature only keeps under an external strain less than approximately -3%. Once the compressive strain exceeds the critical value, the intralayer antiferromagnetic ordering changes to be intralayer antiferromag-

netic, and the interlayer couplings remain antiferromagnetic, known as G-type antiferromagnets. Meanwhile the band gap reduces linearly with respect to the increasing compressive strain strength. Both tensile and compressive strains can be introduced by choosing adjacent 2D materials with larger or smaller lattice constants, the robust antiferromagnetic insulating phase make B_5N_5 a possible building block in 2D vdW spintronic devices.

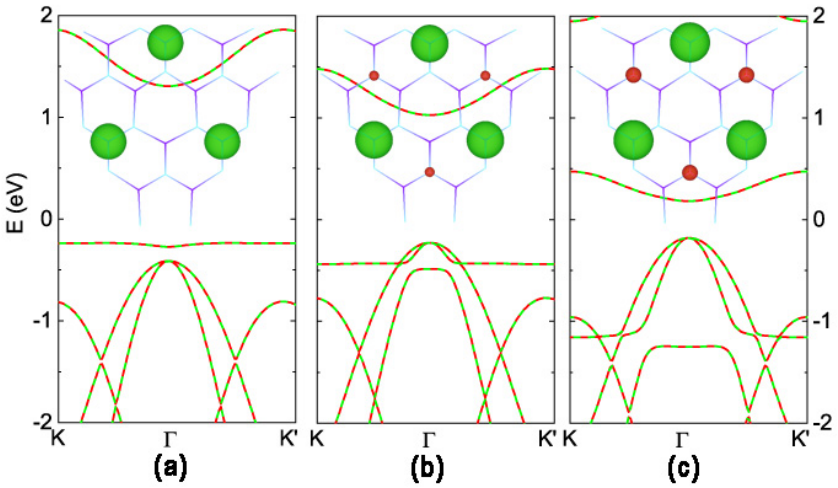

Figure S3: B_5N_5 **monolayers under external strains.** Evolution of band structures under compressive biaxial strains as measured to be (a) -2%, (b) -3% and (c) -5%. The inset pictures illustrate top view of intralayer spin orderings, spatial distributions of spin-up and spin-down states are denoted with green and red spots on lattice, respectively.

4 Part IV. Perpendicular Electric Fields

Perpendicular electric fields are effective to remove the degeneracy of the flat band, and separate spin-up and spin-down channels without overlapping. In FigS.S4, the zoom-in splitting spin state dispersions are shown with continuously increasing external gate voltages. One can find out that,

any perpendicular electric field can remove the spin degeneracy of the flat bands. As the narrow bandwidths of the spin dispersions even under the external electric field, the spin-up and spin-down channels can be separate completely at a relatively small critical gate voltage.

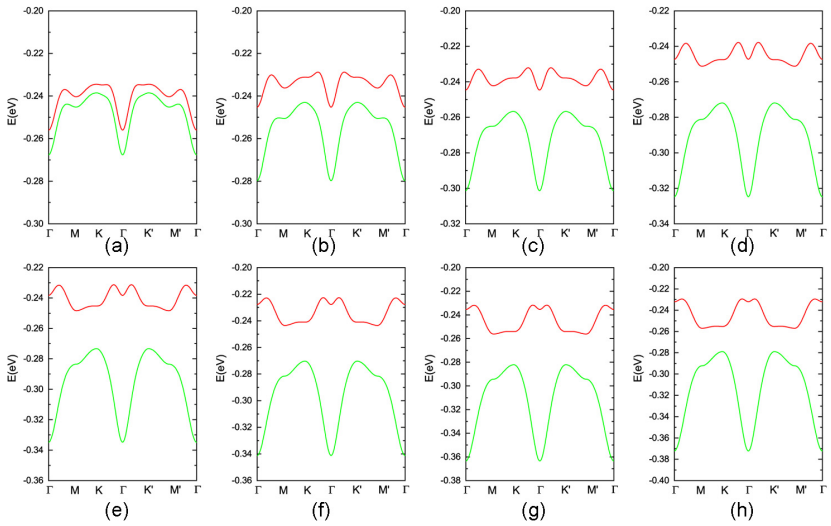

Figure S4: B_5N_5 **monolayers under perpendicular electric fields.** Zoom-in band structures of the splitting spin states in vicinity of the Fermi level. The band structures are shown all over the first Brillouin Zone, and from (a) to (h), the perpendicular gate voltages read 0.2, 0.6, 1.0, 1.4, 1.8, 2.2, 2.6 and 3 V, respectively.

The critical gate voltage reads 0.58 V, and is mapped out by fitting the energy differences between the minimum spin-up states and the maximum spin-down states. From FigS.S5, the purple area indicates the opposite spin channels are completely separated. When the gate voltage exceeds 1.27 V, the spin gaps maintains at a value about 27 meV.

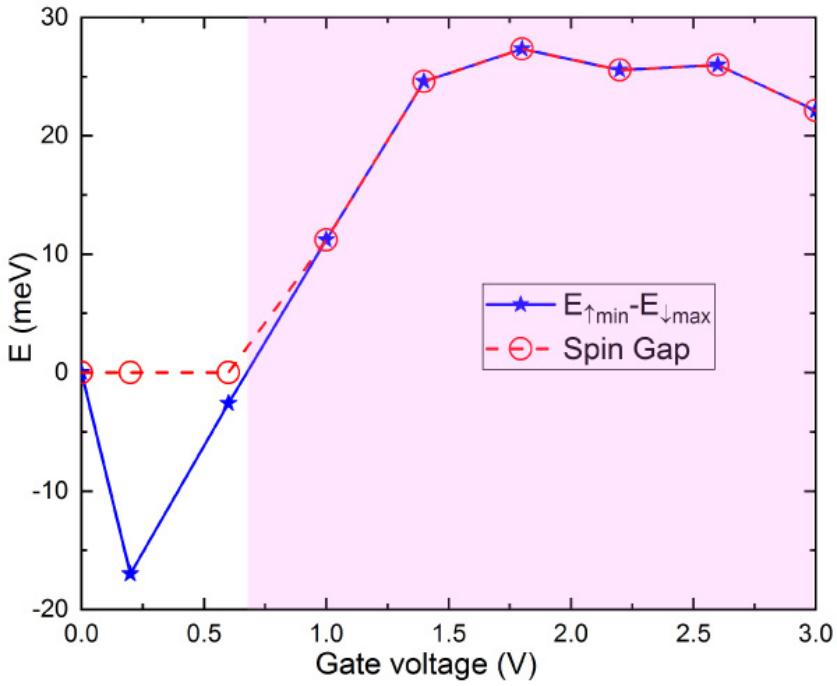

Figure S5: Relationship between $E_{\uparrow min} - E_{\downarrow max}$ (blue solid line with stars), spin gap (red dashed line with circles) and the perpendicular gate voltages. The purple area indicates the opposite spin channels are completely separated.